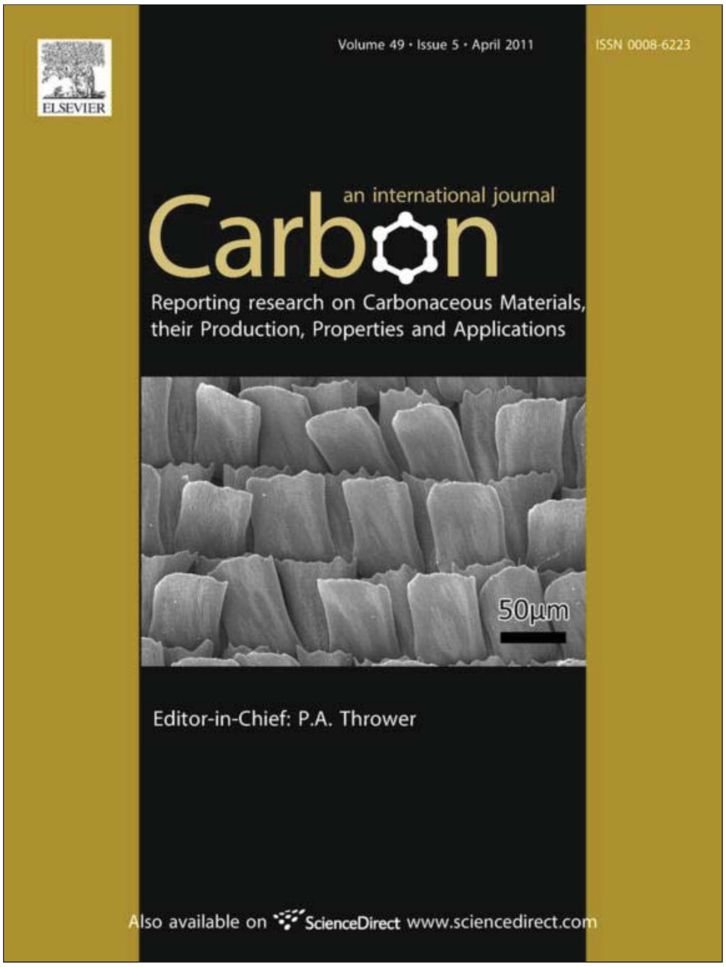
Volume 49 • Issue 5 • April 2011
ISSN 0008-6223
ELSEVIER
an international journal
Carbon
Reporting research on Carbonaceous Materials, their Production, Properties and Applications
50μm
Editor-in-Chief: P.A. Thrower
Also available on ScienceDirect www.sciencedirect.com

CARBON 49 (2011) 1599–1607

available at www.sciencedirect.com

ScienceDirect

journal homepage: www.elsevier.com/locate/carbon

A comparison of the effects of multi-wall and single-wall carbon nanotube additions on the properties of zirconia toughened alumina composites

M.H. Bocanegra-Bernal [a], J. Echeberria [b], J. Ollo [b], A. Garcia-Reyes [c], C. Domínguez-Rios [a], A. Reyes-Rojas [a], A. Aguilar-Elguezabal [a,*]

[a] Centro de Investigación en Materiales Avanzados, CIMAV S.C., Laboratorio Nacional de Nanotecnología, Miguel de Cervantes # 120 Comp. Ind., Chihuahua 31109, Mexico
[b] CEIT and TECNUN (University of Navarra), 20018 San Sebastian, Spain
[c] Interceramic, Dept. of R&D, Av. Carlos Pacheco 7200, Chihuahua 31060, Mexico

ARTICLE INFO

Article history:
Received 26 July 2010
Accepted 13 December 2010
Available online 16 December 2010

ABSTRACT

The use of multi-wall carbon nanotubes (MWCNTs) or single-wall carbon nanotubes (SWCNTs) as filler in ceramic matrices could create composites with exceptional mechanical properties. We have prepared dense monolithic alumina (Al_2O_3) and zirconia-toughened alumina (ZTA) composites with additions of 0.01 wt% of MWCNTs or 0.01 wt% of SWCNTs by conventional sintering and have demonstrated that the mechanical properties depend on (a) the distribution of CNTs in the matrix and (b) the interaction between the ceramic phases and CNTs. The fracture toughness of Al_2O_3 ceramics reinforced with SWCNTs was significantly better than those reinforced with MWCNTs. However, fracture toughness in MWCNT-reinforced ZTA increased 41% over ZTA free of the toughening agent and 44% over ZTA reinforced with SWCNTs. A well dispersed and small amount of MWCNTs was enough to produce an increase of fracture toughness in ZTA composites.

1. Introduction

The processing of nanostructured materials is a part of an emerging field referred to as nanotechnology involving the production of bulk materials with grain size less than 100 nm with excellent properties compared with their micro-crystalline counterparts [1–3]. Although nanocrystalline ceramics have high stiffness and excellent thermal stability with low density, their brittleness impedes the use as structural materials [4]. Sophisticated strategies have been proposed in order to improve the mechanical properties of nanocrystalline ceramics by dispersing nanometer-size second-phase reinforcement to obtain nano-scale composite materials [5,6]. Carbon nanotubes [7] (generally abridged as CNTs) have opened up new technological areas where they can be used as strong, light and high toughness reinforcement fibers for composite structures [8] opening thus the way into nanotechnology [9]. Nanotubes exist as either single-walled (SWCNTs) described by rolling one graphene sheet to form a hollow tube, or multi-walled nanotubes (MWCNTs) simply composed of concentric graphene layers [4,10] and often capped at each end. Depending on synthesis method and conditions, SWCNTs and MWCNTs can be obtained with high structural perfection. The interest of using CNTs in ceramic composites is due to their formidable mechanical properties [11] i.e., Young's modulus up to 1470 GPa for SWCNT [12] and up to 950 GPa for MWCNTs [13]. CNTs with high length/diameter ratio (aspect ratio around 1000 or higher) and small

* *Corresponding author:* Fax: +52 614439 4852.
E-mail addresses: alfredo.aguilar@cimav.edu.mx, alfredo.aguilar@mail.cimav.edu.mx (A. Aguilar-Elguezabal).
0008-6223/$ - see front matter
doi:10.1016/j.carbon.2010.12.042

diameter (no more than one hundred nanometers) have exceptional mechanical characteristics [5,14].

Since the report on MWCNTs made by Iijima [7], the potential for ceramics reinforced with CNTs having extraordinary stiffness and strength represent an important step in the development of ceramic composites with improved fracture toughness and strength over monolithic ceramic materials [15]. A lot of research work on carbon nanotubes reinforced composites has concentrated on polymer-matrix materials for improved electric conductivity, optical devices and higher strength [8]. There are few studies carried out on CNTs reinforced metals and the use of carbon nanotubes as reinforcement in ceramics has not been very successful [16]. For example, An et al. [17] studied the influence of CNTs content on the tribological properties of CNTs/Al_2O_3 composites and reported an increase in microhardness of 30% more than pure Al_2O_3; Siegel et al. [18] obtained an increase in fracture toughness about 24% in alumina reinforced with 10 vol % MWCNTs. More recently, Zhan et al. [5] reported a fracture toughness of 9.7 MPa $m^{1/2}$ with an Al_2O_3/10 vol % SWCNTs composite, nearly three times that of nanocrystalline alumina at sintering temperatures as low as 1150 °C by spark plasma sintering (SPS). Wang et al. [19] have used SPS to densify Al_2O_3 reinforced with also 10 vol % SWCNT obtaining densities of 95% and fracture toughness of 3.32 MPa $m^{1/2}$. This, compared with indentation toughness of dense pure Al_2O_3 of 3.3 MPa $m^{1/2}$ clearly show that, within experimental scatter, the fracture toughness values of the two materials is the same. On the other hand, Peigney et al. [20] in very recent investigation obtained an increase in both toughness and microhardness in double-walled carbon nanotubes (DWCNTs)/nanostructured magnesia composites. Most of the investigations have focused mainly on alumina-based ceramic composites [21] using both SWCNTs and MWCNTs but unambiguous demonstration of toughening in these composites remains elusive.

Carbon nanotubes may result in an entire new class of advanced materials [15] exploiting their excellent mechanical properties leading to ceramic/SWCNTs or ceramic/MWCNTs that are both tough and strong [22]. There are challenges to obtain uniform dispersion of very high concentrations of CNT (for example 10 vol % used in several investigations [5,18,22]) as well as to explore in detail the control of the interface between the nanotubes and the matrix [4], so that they actually carry the loads [5]. SWCNT are preferred inasmuch as some authors report, MWCNT could exhibit very easy interwall sliding, with inner graphitic walls able to be extracted from outer walls in a 'sword and sheath' failure, where outermost layer in the MWCNT breaks followed by pull out of the inner shells [5] contributing little to carrying load. However, a problem exists in SWCNT where often are formed close-packed bundles or ropes bound by weak van der Waals interaction that can easily slide with respect to each other. Therefore, this inter-bundle slippage limits the load-bearing of SWNT, so their mechanical performances are far below that of individual CNTs [23]. An effective prevention of slide between the bundles or ropes, through the formation of stable links between SWCNT for improvement of mechanical properties is required according to Yamamoto et al. [24].

In order to obtain comparative results on the use of SWCNTs and MWCNTs as ceramic reinforcement additives, in this work we have used a very low amount of SWCNTs and MWCNTs to obtain considerable reinforcement in the pressureless sintered ceramic composites based Al_2O_3 (Zirconia Toughened Alumina (ZTA)) and determine which of the two reinforcement agents has higher contribution to the unusual mechanical properties.

2. Experimental methods

2.1. Materials

High purity α-Al_2O_3 (Baikalox SM8, Baikowski, USA; primary particle size 50 nm, purity > 99.99%, surface area 10 $m^2\,g^{-1}$), MgO (500A, UBE Chemical Industries, Japan; primary particle size 53 nm, purity > 99.999%, surface area 32 $m^2\,g^{-1}$), ZrO_2 + 3 mol% Y_2O_3 (abridged as TZ-3Y, Tosoh, Japan; primary particle size 75 nm, purity > 99.99%, surface area 17 $m^2\,g^{-1}$), monoclinic ZrO_2 (Aldrich, USA; primary particle size < 50 nm, purity > 99.99%, surface area 15–35 $m^2\,g^{-1}$) powders, MWCNT (Catalysis Laboratory of CIMAV S.C. [25]), diameter 70–110 nm, length 120–160 μm, purity > 95%, surface area 25 $m^2\,g^{-1}$, and high purity SWCNT (HELIX Material Solutions), diameter ~ 1.3 nm, length 0.5–40 μm, purity > 90 %, and surface area > 300 $m^2\,g^{-1}$ were used as starting materials.

2.2. Mixture

Homogeneous mixtures of Al_2O_3 + 0.025 wt% MgO + 13 wt% TZ-3Y + 2 wt% $ZrO_{2(m)}$ with additions of 0.01 wt% of MWCNTs and SWCNTs were prepared. A composite without additions of MWCNTs and SWCNTs as well as samples of pure Al_2O_3 and Al_2O_3 with additions of 0.01 wt% MWCNTs and SWCNTs were also prepared as comparison. In order to illustrate the dispersion of great concentrations of MWCNTs and SWCNTs, mixtures of ZTA with additions of 10 vol % of MWCNTs and SWCNTs were also prepared following the same steps. Care has been taken to mix the nanopowders with MWCNTs and SWCNTs. The as-received MWCNTs and SWCNTs were carefully dispersed in 500 mL ethanol with ultrasonic agitation for 2 h. Nanopowders and the dispersed MWCNTs or SWCNTs in alcohol media were vigorously stirred until most of ethanol evaporated and then the mixture was dried at 100 °C for 12 h. The agglomerated mixture was ground intense and carefully in an agate mortar.

2.3. Processing

Approximately 2 g of each mixture was uniaxially pressed at 50 MPa in a disk (steel die) with 16 mm diameter and 7 mm height using an Elvec Hydraulic Press at a constant strain rate. Green samples with additions of MWCNTs and SWCNTs were confined into an alumina sagger with high purity graphite packing powder (graphite powder, crystalline, −300 mesh, 99%, Alfa Aesar), where the alumina powder fill the space between the two high alumina crucibles. A third crucible covers the one containing the graphite bed powder with the sample. Samples without additions of MWCNTs and SWCNTs were directly set into Al_2O_3 crucible with ZrO_2 + Al_2O_3 bed powder. All samples were sintered at 1520 °C during 1 h in air at a heating rate of 10 °C m^{-1}. After sintering, the furnace was shut off and it was allowed to cool down. Density was measured by means of Quantachrome Multipycnometer using Helium as displacement gas for the as-sintered composites. The samples were ground and polished by SiC paper and then polished by diamond pastes of both 0.5 and 0.25 μm. Samples were thermally etched at 1370 °C for 30 min, following the same procedure for sintering so as to preserve the carbon nanotubes. Each experiment was made four times.

2.4. *Characterization*

The polished and fracture surfaces were characterized by scanning electron microscopy (SEM: JEOL JSM 5800 LV, Japan, and FEG SEM: JEOL JMS 7000F, Tokyo, Japan) using an accelerating voltage of 2 kV. A small amount of MWCNTs and SWCNTs were dispersed onto a TEM grid to be characterized by transmission electron microscopy (TEM: HRTEM JEM 2200 FS). The average grain size in pure ZTA and ZTA/0.01 wt% MWCNT composite was measured using the linear intercept technique using 300–400 grains for each sample. Raman spectra were obtained with Thermo Nicolet Almega XR Dispersive Raman Spectrometer (λ_{ex} = 532 nm and maximum power 20 mW).

2.5. *Mechanical properties*

Vickers hardness measurements were carried out on the sintered samples using FM-7 microhardness tester. Three samples per composition (diameter 12 mm, thickness 6 mm) and approximately 20–30 indents per each measurement were made on polished surfaces with a load of 1 kg held for 15 s and an average hardness was determined. The separation between neighboring indentations was more than four diagonal lengths of indentation impression according to the standard ASTM C1327-99 for Vickers indentation hardness of advanced ceramics [26]. With the help of an optical microscope Olympus PMG3, the corresponding indentations sizes and crack lengths were measured soon after indentation to prevent the slow crack growth associated with the stress field that acts after removal of indenter and with the environmental effect. The indentation fracture toughness (K_{IC}) was derived from average crack length. For a ratio $c/a > 2.5$ (present study), where c is the crack length and a corresponds to the half diagonal length of the indentation impression, K_{IC} was calculated using the equation derived by Evans and Charles [27].

3. Results and discussion

3.1. *Composite powders*

The Fig. 1a is a typical transmission electron micrograph (TEM) showing the nanostructure of a MWCNTs with a few nanometer in diameter where a hollow core and several layers of graphitic carbon are aligned corresponding to the final step of the formation mechanism of MWCNTs. SWCNT tend to assemble in 'ropes' of nanotubes as can be seen in Fig. 1b which consist of typically 5–7 tubes with diameter < 3 nm and aligned along their length in van der Waals bonding with one another (Fig. 1c, high magnification square from Fig. 1b) . A lack of concentric ring patterns indicates the absence of MWCNTs. Diameter of SWCNTs is below 5 nm and length of less than 5 microns while in the case of MWCNTs, their characteristics may vary in a wide set of values. MWCNT synthesized in our team group present a diameter and length of 80–100 nm and 150 ± 25 μ, respectively.

3.2. *Sintered materials*

To investigate the mechanical behavior of ZTA ceramic composite, we prepared our own high-density ZTA/0.01 wt% MWCNTs and SWCNTs composites using conventional sintering at 1520 °C during 1 h. Pure ZTA composite free of carbon nanotubes additions and pure Al_2O_3, and Al_2O_3 reinforced with 0.01 wt% MWCNTs and SWCNTs were also prepared for comparison alone. The densities of the six materials processed in this investigation are summarized in Table 1. It can be seen that pure alumina, reinforced and without reinforcement as well as the ZTA composites with and without additions of CNTs are consolidated at approximately the same sintered density considering the experimental dispersion. The fracture surfaces of carbon nanotubes reinforced alumina composites are shown in Fig. 2a for Al_2O_3/0.01 wt% MWCNTs and Fig. 2b for Al_2O_3/0.01 wt% SWCNTs, respectively. As can be seen, SWCNTs (Fig. 2b) were distributed inside the alumina grains and strongly bonded with the alumina matrix (see arrows marks), and even a hole resulting from a CNT pull-out can be observed (see circle mark). On the other hand, the MWCNTs are located mainly in the intergranular places making the boundaries mechanically weak causing mainly fracture along the grain boundaries as can be seen in Fig. 2a. In this context, the strengthening and toughening mechanisms show that SWCNTs perpendicular to the fracture surfaces can contribute significantly to improve the mechanical properties (see high magnification inserts of squares in Fig. 2b). This appreciation could be supported with the Fig. S1 in Supplementary material, where at higher magnification of one arm of a Vickers hardness impression (see Fig. S1b in Supplementary material), the evidence of crack deflection as well as bridging effect of carbon nanotubes during crack propagation (arrow marks), and CNT pull-out (circle) (see Fig. S1c in Supplementary material) are clearly observed.

Scanning electron micrographs (SEM) of fracture surfaces of pure ZTA, ZTA/0.01 wt% MWCNTs and ZTA/0.01 wt% SWCNTs composites are shown in Fig. S2a–c, in Supplementary material. Intergranular fracture accompanied by partial transgranular fracture can be observed in the three samples being predominant transgranular fracture mode in ZTA/0.01 wt% SWCNTs composite. It is scarce to find CNTs due to the low content as only 0.01 wt%, which is quite similar to the reported by Sun et al. [28]. The preservation of CNT after sintering process was confirmed by Raman spectroscopy and as can be seen in Fig. 3, typical Raman absorption signals for MWCNTs and SWCNTs appear in their correspondent spectra. These spectra were taken from fracture surfaces.

3.3. *Mechanical properties*

Although the fracture toughness determined by the Vickers indentation fracture method has been widely used due to

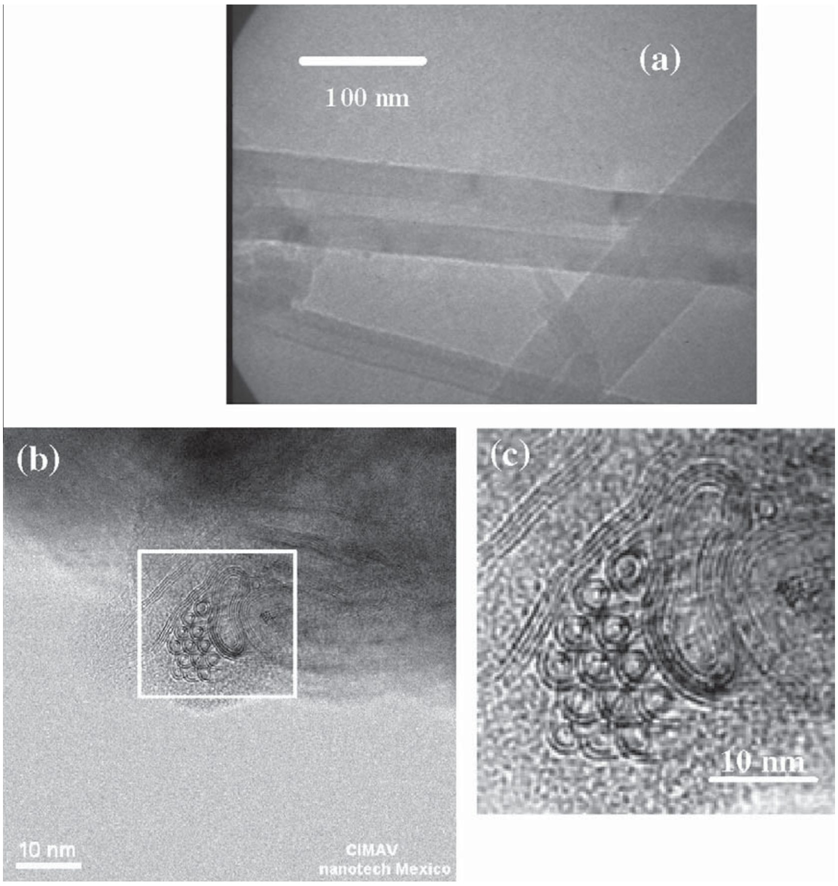

Fig. 1 – Transmission electron micrographs (TEM) of (a) MWCNT, and (b) SWCNT. High magnification of the square in (b) is shown in (c).

Table 1 – Densities corresponding to the experimental materials.

Sample	Sintering		Measured density ($g\,cm^{-3}$)	Theoretical density ($g{\cdot}cm^{-3}$)	Relative density (%)
	Temperature (°C)	Time (h)			
Pure ZTA	1520	1	4.15	4.29	96.71
ZTA/0.01 wt% MWCNTs	1520	1	4.12	4.29	96.00
ZTA/0.01 wt% SWCNTs	1520	1	4.10	4.29	95.46
Pure Al_2O_3 (SM8)	1520	1	3.89	3.98	97.56
Al_2O_3/0.01 wt% MWCNTs	1520	1	3.79	3.98	95.24
Al_2O_3/0.01 wt% SWCNTs	1520	1	3.78	3.98	94.96

its ease of use, it has not been widely accepted due to the complexity of the stress fields involved in the Vickers indentation, and taking into account that an economical and effective technique to characterize the fracture toughness in ceramics is currently not available [29], considerable care must be used to measure the length of the cracks. Vickers indentation test on our composites showed clear evidence of classical radial cracking and considering that these were well-defined, we can readily calculate the fracture toughness using Evans and Charles equation [27]. Similar procedures were reported by Zhan et al. [5]. In the case of complete absence of classical radial cracks, the fracture toughness measurement using Vickers indentation test could not be valid [19].

SEM micrographs of typical Vickers indentation in pure ZTA, ZTA/0.01 wt% MWCNTs, and ZTA/0.01 wt% SWCNTs, are shown in Fig. 4a–c, respectively. The length of crack is smaller in ZTA/0.01 wt% MWCNTs (Fig. 4e) indicating a higher fracture toughness in comparison to pure ZTA and ZTA/0.01 wt% SWCNTs (Fig. 4d and f). Conditions of processing and mechanical properties for the composites are shown in Table 2. It is observed that the measured Vickers hardness remains approximately constant for pure ZTA and CNTs reinforced ZTA composites. Fracture toughness for MWCNTs reinforced ZTA composites was 41% and 44% over ZTA free of toughening agent and over ZTA reinforced with SWCNT, respectively. Conversely, the fracture toughness for MWCNT and SWCNT reinforced Al_2O_3 ceramic was 9% lower and 12%

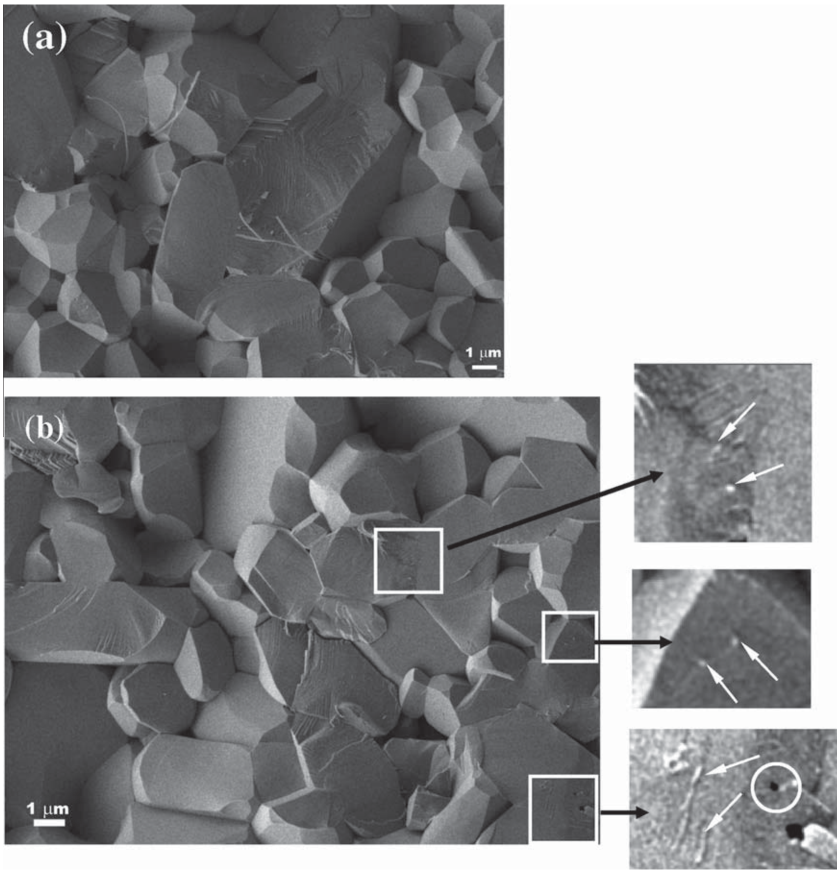

Fig. 2 – SEM micrographs of fracture surfaces of (a) Al_2O_3/0.01 wt% MWCNT, (b) Al_2O_3/0.01 wt% SWCNT. Arrow marks and circle are explained in text.

higher than monolithic Al_2O_3, respectively. A different behavior of CNT in monolithic Al_2O_3 is clear, compared to ZTA composites for the same CNT content. As was mentioned earlier, although some reliability problems pertaining to the fracture toughness measured by Vickers indentation in ceramics, the resulting toughening effect of 41% and 44% deserves merit as a relative measurement of the fracture toughness [30].

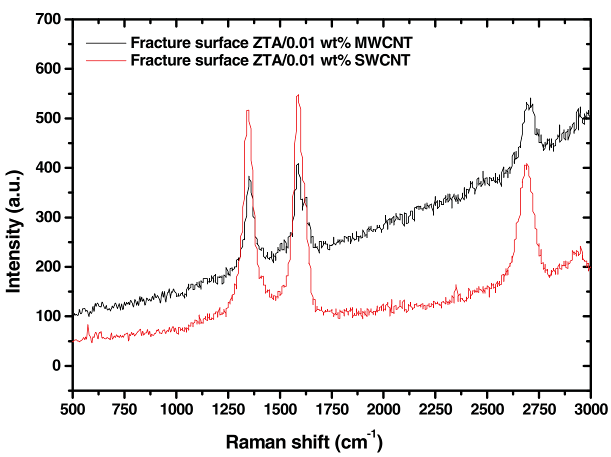

Fig. 3 – Raman spectra of ZTA/0.01 wt% MWCNT and ZTA/ 0.01 wt% SWCNT.

Observations at higher magnification of a segment of the crack emerging from the indentation corner and denoted as 1 in pressureless sintered (Fig. 4a–c) of pure ZTA, MWCNT and SWCNT reinforced ZTA composites, respectively, showed inter and intragranular fracture (see Fig. S3 in Supplementary material). Predominant intergranular fracture (crack deflection where the crack front interacts with a second-phase and changes its propagation path altering the fracture mode from pure mode I [31]) was clearly evident in ZTA/0.01 wt% MWCNT (circles in Fig. S3b in the Supplementary material). When fracture occurs intergranularly, the fracture energy is expected to scale approximately linearly with the grain size [32], being more tortuous for a material with larger grain size, (0.53 ± 0.25 μm for ZTA/0.01 wt% MWCNT composite vs 0.46 ± 0.21 μm for pure ZTA composite). As a result, the crack path tortuosity increases dramatically with increasing grain size and therefore, the crack roughness is slightly greater in ZTA/0.01 wt% MWCNT (see Fig. S2b in Supplementary material) composites compared to the pure ZTA (Fig. S2a in Supplementary material) and ZTA/0.01 wt% SWCNT (see Fig. S2c in Supplementary material). The crack is characterized by a small number of deviations at large angles and therefore, a very tortuous path occurs explaining the high efficiency of the deflection mechanism and therefore, an increase in fracture toughness (Fig. S3b in Supplementary material). MWCNT pull-outs were also detected on the fracture surface (see arrow marks in Fig. S2d in Supplementary material) suggesting

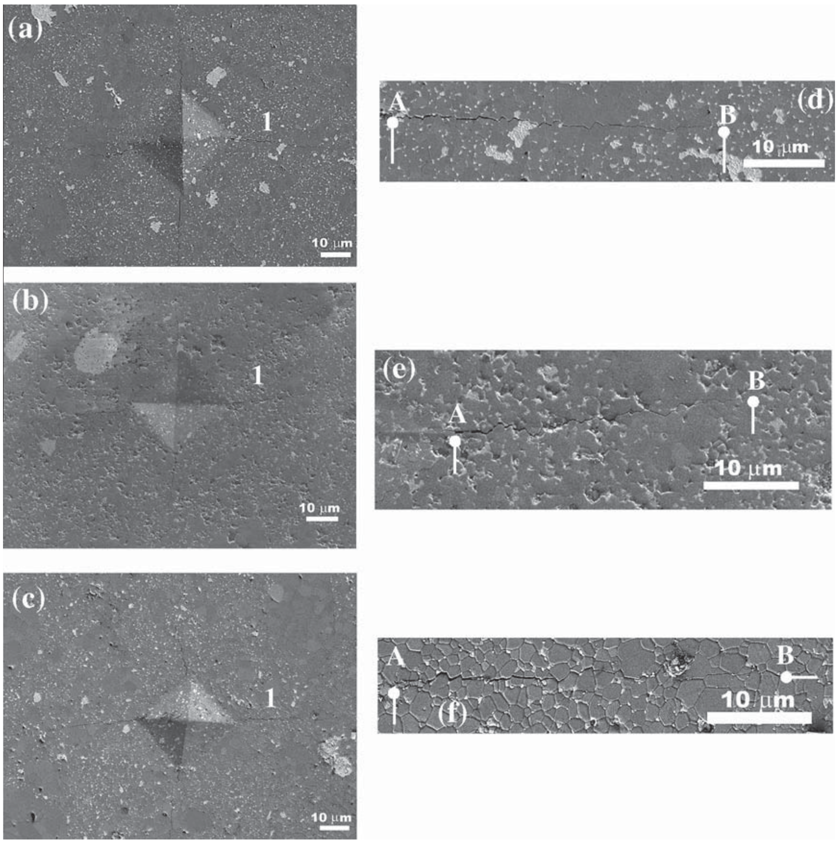

Fig. 4 – Scanning electron micrographs (SEM) of 10 N Vickers indentations in (a) Pure ZTA, (b) ZTA/0.01 wt% MWCNT, (c) ZTA/0.01 wt% SWCNT composites. (d-f) corresponds to high magnification of the cracks denoted as 1 in (a-c). A and B in d-f corresponds to the beginning and end of the crack length.

Table 2 – Mechanical properties of the experimental materials.

Sample	Sintering		Hardness (GPa)	Fracture toughness (MPa $m^{1/2}$)
	Temperature (°C)	Time (h)		
Pure ZTA	1520	1	16.12 ± 0.49	3.32 ± 0.11
ZTA/0.01 wt% MWCNTs	1520	1	15.66 ± 0.87	4.68 ± 0.55
ZTA/0.01 wt% SWCNTs	1520	1	17.10 ± 0.51	3.25 ± 0.44
Pure Al_2O_3 (SM8)	1520	1	17.20 ± 1.27	3.34 ± 0.39
Al_2O_3/0.01 wt% MWCNTs	1520	1	15.49 ± 0.98	3.05 ± 0.19
Al_2O_3/0.01 wt% SWCNTs	1520	1	14.60 ± 0.68	3.73 ± 0.53

a strong bonding between CNT and Al_2O_3 matrix and significant load transfer from the matrix to carbon nanotubes during loading [33]. Considering the sintering conditions applied during the processing of composite, the outer wall of CNT comprise a graphitic wall where chemical interaction with ceramic structure is not possible, thus load transfer under stress corresponds to a physical process where morphology of CNTs is fundamental, and mainly depends on interfacial surface, roughness of CNTs surface, and diameter/length ratio. A more magnified case is illustrated in Fig. S4 in Supplementary material where simultaneously MWCNT pull-out and its debonding from the alumina matrix leaving traces ("footprints") on the fracture surface took place, supporting also, the crack deflection mechanism, which is consistent with Fig. S3b, in the Supplementary material. The white arrow marks in Fig. S4 indicate the position where the MWCNT pull-out changed in diameter along the fragment until breakage of the CNT, suggesting an effective frictional resistance between the CNT and the alumina matrix. On the other hand, the black arrows in Fig. S4 illustrate the "footprints" corresponding to exposed length of the MWCNT. Similar behavior was observed by Yamamoto et al. [34] in acid-treated MWCNT/alumina composite. Conversely, lower fracture toughness in pure ZTA (see Fig. S3a in Supplementary material) and ZTA/0.01 wt% SWCNT (Fig. S3c in Supplementary material) can be explained by the decreasing in number of crack deviations as well as deflection angles indicating that crack deflection mechanism is less effective in the toughening process [35]. In intergranular fracture the crack propagates along the grain boundary thus consumes more fracture energy, which is favorable for the increment of fracture toughness [36]. The fraction of intragranular fracture mode dominates only when the strength of the grain boundary is close to that of the matrix grain. Therefore, strongly bonded CNT make the matrix fracture through the grains rather than intergranulary, as prevails commonly in monolithic Al_2O_3 [37].

Considering the higher aspect ratio and greater surface area in SWCNT than MWCNT it is suggested that more interfacial bonding is present. Interfacial bonding would be an important factor to take into account to increase the toughness in the composites [5]. However, too good interfacial bonding would make the ceramic too brittle [38] which could occur with higher concentration of CNT where the grain growth and congregation of alumina grains during sintering process can be greatly inhibited leading to detrimental grain boundary cohesion [20]. This appreciation can be supported with the fracture surfaces of our sintered ZTA reinforced with 10 vol % MWCNT and 10 vol % SWCNT composites illustrated in the Fig 5a and b, respectively. From these images one can find that the composites reinforced with large CNTs content affect the sintering ability leading to a poor densification (40% and 60% of theoretical density for Al_2O_3 reinforced with 10 vol % MWCNTs (Fig. 5a) and 10 vol % SWCNTs (Fig. 5b), respectively). On the other hand, for the same nanotubes content, the MWCNTs were homogeneously dispersed meanwhile agglomerates of SWCNTs were formed (arrow in Fig. 5b). Similar observations have been reported by Zhang et al. [39] in CNTs-Al_2O_3 with variable CNTs content and Zhang et al. [40] in alumina ceramics with additions of 1, 3, and 5 vol % MWCNTs. Thus, a too high CNTs content must be avoided. It has been argued that better mechanical properties could result from higher nanotube volume content and, in some cases, the use of longer nanotubes. However, these variations will create additional processing challenges inasmuch as it is very difficult to obtain a uniform dispersion of nanotubes and therefore, to obtain a dense matrix [4].

For the same single-wall and multi-wall carbon nanotubes content in the ZTA composite, the great increase in fracture toughness in MWCNTs reinforced ZTA composite indicates that fiber toughening by MWCNTs is dominant. The best reinforcement with MWCNTs can be due to a better dispersion of these inside the grains of ZTA (see Fig. S2d in Supplementary material) and to a strong bond with alumina matrix. Meanwhile, a decrease in fracture toughness is observed when the distribution of SWCNTs has been preferably at grain boundaries and might be due to the poor adhesion of CNT with this specific matrix [41] and even to an agglomeration of CNTs (Fig. S2c in Supplementary material) which could facilitate the separation from the matrix as consequence of poor load carrying when the stresses transfer to the carbon nanotubes [42]. Cha et al. [43] and Zhan et al. [5] have also reported the agglomeration state of carbon nanotubes.

With the mixing method used in this work, where oxides particles and CNTs are suspended in a solvent, and since particle size of all oxides are in the same range (50–75 nm), differences found on MWCNTs and SWCNTs dispersion at sintered composites can be explained for the different surface charge of oxides. The effect of surface charge nature of Al_2O_3, ZrO_2, TZ-3Y and MgO may induce selective covering of specific particles on CNT for ZTA composites (additionally, the difference on MWCNTs and SWCNTs diameter must be taken into account), and this phenomena does not occur for pure Al_2O_3.

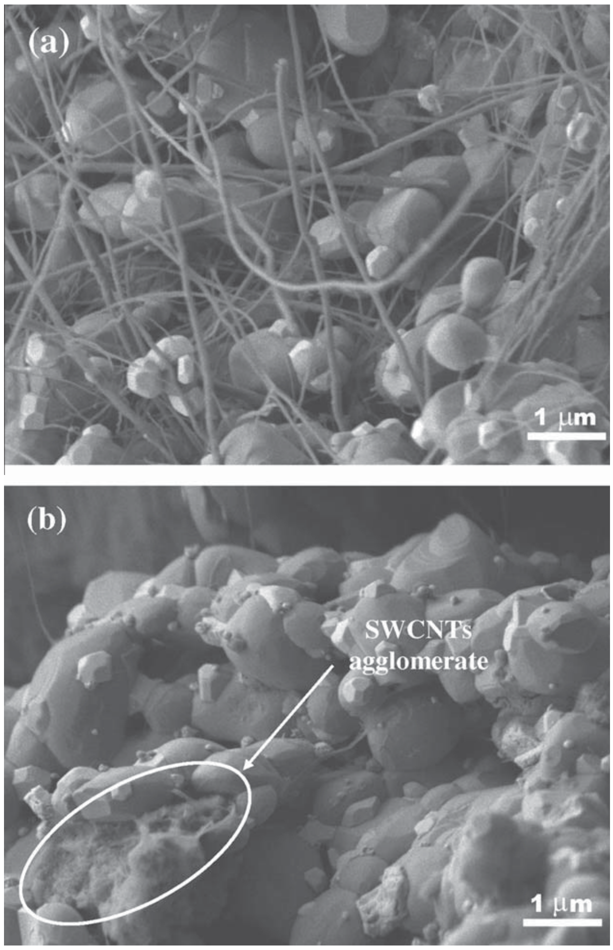

Fig. 5 – SEM of fracture surfaces of ZTA reinforced with (a) 10 vol % MWCNT (40% of theoretical density) and (b) 10 vol % SWCNT (60 % of theoretical density) sintered at 1520 °C during 1 h, showing agglomeration of SWCNT in (b).

4. Conclusion

Contradictory results are published for the use of CNTs as toughening agent. From our results we can conclude that CNTs content on values higher than 4 wt% for alumina based ceramics does not allow the sintering, for this reason, ceramics with low relative density and poor mechanical properties are obtained despite a high CNT dispersion, independently of the use of MWCNT or SWCNT. Results published by other authors with such composition only can be explained by a mechanical work made to disperse the CNTs, where degradation of CNT integrity is produced. Improvement of mechanical properties on alumina based ceramics can be obtained with CNTs content as low as 0.01 wt%. The performance of MWCNTs and SWCNTs as toughening agent of this kind of ceramic oxide composites depends on several variables like dispersion method, nature of matrix, surface charges of particles and particle size distribution as well as diameter and length of CNTs. Thus depending on the above mentioned considerations, the best toughening agent can be different for each specific ceramic composition.

Acknowledgements

The authors would like to thank Professor Amiya K. Mukherjee (University of California) for his continuous support and fruitful discussion. The authors are grateful to Wilber Antu-nez, Karla Campos and Alfredo Nevá rez for assistance in SEM and mechanical properties and to Carlos Ornelas for TEM assistance. It is a pleasure to acknowledge the help of PhD Verónica González Peña and PhD Maria Elena Llanos Serrano from Instituto Mexicano del Petróleo for Raman spectroscopy studies.

Appendix A. Supplementary data

Supplementary data associated with this article can be found, in the online version, at doi:10.1016/j.carbon.2010.12.042.

REFERENCES

[1] Vasylkiv O, Sakka Y, Skorokhod VV. Low-temperature processing and mechanical properties of zirconia and zirconia-alumina nanoceramics. J Am Ceram Soc 2003;86(2):299–304.
[2] Gleiter H. Mechanical Properties and Deformation Behavior of Materials Having Ultra-fine Microstructures. Netherlands: Kluwer Academic; 1993.
[3] Mayo MJ. Mechanical properties and deformation behavior of materials having ultra-fine microstructures. Netherlands: Kluwer Academic; 1993.
[4] Samal SS, Bal S. Carbon nanotube reinforced ceramic matrix composite-a review. J Min Mater Char Eng 2008;7(4):355–70.
[5] Zhan G-D, Kuntz JD, Wam J, Mukherjee AK. Single-wall carbon nanotubes as attractive toughening agents in alumina-based nanocomposites. Nat. Mater. 2003;2(1):38–42.
[6] Wang X, Tian J, Yu X, Shan Y, Liu Z, Yin Y. Effect of microstructure of the fracture behavior of micro-nano ZTA composite. Mater Chem Phys 2008;112(1):213–7.
[7] Iijima S. Helical microtubules of graphitic carbon. Nature 1991;354(6348):56–8.
[8] Sun J, Iwasa M, Nakayama T, Niihara K, Gao L, Jin X. Pressureless sintering of alumina carbon nanotubes composites in air atmosphere furnace and their mechanical properties. J Ceram Soc Jpn Supplement 2004;112(5):S403–6 [Special Issue].
[9] Hammel E, Tang X, Trampert M, Schmit T, Mauthner K, Eder A, et al. Carbon nanofibers for composite applications. Carbon 2004;42(5–6):1153–8.
[10] Peigney A, Laurent CH, Flahaut E, Rousset A. Carbon nanotubes in novel ceramic matrix nanocomposites. Ceram Int 2000;26(6):677–83.
[11] Wong EW, Sheehan PE, Lieber CM. Nanobeam mechanics: elasticity, strength, and toughness of nanorods and nanotubes. Science 1997;277(5334):1971–5.
[12] Yu M, Files BS, Arepali S, Ruoff RS. Tensile loading of ropes of single wall carbon nanotubes and their mechanical properties. Phys Rev Lett 2000;84(24):5552–5.
[13] Yu M, Lourie O, Dyer MJ, Moloni K, Kelly TF, Ruoff RS. Strength and breaking mechanism of multiwalled carbon nanotubes under tensile load. Science 2000;287(5453):637–40.
[14] Zhu Y-F, Shi L, Liang J, Hui D, Lau K-t. Synthesis of zirconia nanoparticles on carbon nanotubes and their potential for enhancing the fracture toughness of alumina ceramics. Compos. Part B 2008;39(7–8):1136–41.
[15] Thostenson ET, Ren Z, Chou T-W. Advances in the science and technology of carbon nanotubes and their composites: a review. Comp Sci Tech 2001;61(13):1899–912.
[16] Fan J, Zhao D, Wu M, Xu Z, Song J. Preparation and microstructure of multi-wall carbon nanotubes-toughened Al_2O_3 composite. J Am Ceram Soc 2006;89(2):750–3.
[17] An JW, You DH, Lim DS. Tribological properties of hot-pressed alumina-CNT composites. Wear 2003;255(1–6):677–81.
[18] Siegel RW, Chang SK, Ash BJ, Stone J, Ajayan PM, Doremus RW, et al. Mechanical behavior of polymer and ceramic matrix nanocomposites. Scr Mater 2001;44(8–9):2061–4.
[19] Wang X, Padture NP, Tanaka H. Contact-damage-resistant ceramic/single-wall carbon nanotubes and ceramic/graphite composites. Nat Mater 2004;3(8):539–44.
[20] Peigney A, Legorreta García F, Estournès C, Weibel A, Laurent C. Toughening and hardening in double-walled carbon nanotube/nanostructured magnesia composites. Carbon 2010;48(7):1952–60.
[21] Duszova A, Dusza Jan, Tomasek K, Morgiel J, Blugan G, Kuebler J. Zirconia/carbon nanofiber composite. Scr Mater 2008;58(6):520–3.
[22] Padture NP. Muntifunctional composites of ceramics and single-walled carbon nanotubes. Adv Mater 2009;21(17):1767–70.
[23] Kis A, Csányi G, Salvetat J-P, Lee T-N, Couteau E, Kulik AJ, et al. Reinforcement of single-walled carbon nanotube bundles by intertube bridging. Nature 2004;3(3):153–7.
[24] Yamamoto G, Sato Y, Takahashi T, Omori M, Hashida T, Okubo A, et al. Single-walled carbon nanotube-derived novel structural material. J Mater Res 2006;21(6):1537–42.
[25] Aguilar-Elguézabal A, Antunez W, Alonso G, Paraguay F, Espinosa F, Miki-Yoshida M. Study of carbon nanotubes synthesis by spray pyrolysis and model of growth. Diamond Rel Mater 2006;15(9):1329–35.
[26] ASTM C-1327-99. Standard test method for Vickers indentation hardness of advanced ceramics. Annual Book of ASTM Standards, vol. 14.02, 1999.
[27] Evans AG, Charles EA. Fracture toughness determination by indentation. J Am Ceram Soc 1976;59(7–8):371–2.
[28] Sun J, Gao L, Iwasa M, Nakayama T, Niihara K. Failure investigation of carbon nanotube/3Y-TZP nanocomposites. Ceram Int 2005;31(8):1131–4.
[29] Jiang D, Mukherjee AK. Response to comment on "effect of sintering temperature on single-wall carbon nanotube toughened alumina-based nanocomposite". Scr Mater 2008;58(11):991–3.
[30] Kim SW, Chung WS, Sohn K-S. Son Ch-Y, Lee S. Improvement of wear resistance in alumina matrix composites reinforced with carbon nanotubes. Matall Mater Trans A 2010;41(2):380–7.
[31] Gatto A. Critical evaluation of indentation fracture toughness measurements with Vickers indenter on ceramic matrix composite tools. J Mater Proc Tech 2006;174(1–3):67–73.
[32] Kovar D, Bennison SJ, Readey MJ. Crack stability and strength variability in alumina ceramics with rising toughness-curve behavior. Acta Mater 2000;48(2):565–78.
[33] Mo ChB, Cha SI, Kim KT, Lee KH, Hong SH. Fabrication of carbon nanotube reinforced alumina matrix nanocomposite by sol-gel process. Mater Sci Eng 2005;A395(1–2):124–8.
[34] Yamamoto G, Omori M, Hashida T, Kimura H. A novel structure for carbon nanotube reinforced alumina composites with improved mechanical properties. Nanotechnology 2008;19:315–708.

[35] Celli A, Tucci A, Esposito L, Palmonari C. Fractal analysis of crack in alumina-zirconia composites. J Eur Ceram Soc 2003;23(3):469–79.
[36] Teng X, Liu H. Huang Ch. Effect of Al_2O_3 particle size on the mechanical properties of alumina-based ceramics. Mater Sci Eng 2007;A452–A453:545–51.
[37] Ahmad I, Cao H, Chen H, Zhao H, Kennedy A, Qiu Zu Y. Carbon nanotube toughened aluminum oxide nanocomposite. J Eur Ceram Soc 2010;30(4):865–73.
[38] White AA, Best SM, Kinloch AA. Hydroxyapatite-carbon nanotube composites for biomedical applications: a review. Int J Appl Ceram Technol 2007;4(1):1–13.
[39] Zhang T, Kumari L, Du GH, Li WZ, Wang QW, Balani K, et al. Mechanical properties of carbon nanotube-alumina nanocomposites synthesized by chemical vapor deposition and spark plasma sintering. Compos Part A 2009;40(1):86–93.
[40] Zhang SC, Fahrenholtz WG, Hilmas GE, Yadlowsky EJ. Pressureless sintering of carbon nanotube-Al_2O_3 composites. J Eur Ceram Soc 2010;30(6):1373–80.
[41] Vasilev AL, Poyato R, Padture NP. Single-wall carbon nanotubes at ceramic grain boundaries. Scr Mater 2007;56(6):461–3.
[42] Ahmad K, Pan W. Hybrid nanocomposites: a new route towards tougher alumina ceramics. Comp Sci Tech 2008;68(6):1321–7.
[43] Cha SI, Kim KT, Mo CB, Hong SH. Strengthening and toughening of carbon nanotube reinforced alumina nanocomposite fabricated by molecular level mixing process. Scr Mater 2005;53(7):793–7.